

# Optimized HVOF Titania Coatings

R.S. Lima and B.R. Marple

(Submitted 1 May 2002; in revised form 31 August 2002)

A series of spray parameters was tested for a titania ( $\text{TiO}_2$ ) feedstock, and the in-flight particle temperature was measured for each setting combination. The parameter set that resulted in the highest particle temperature was selected for producing coatings for further study and analysis. With this parameter set, the majority of the sprayed particles had temperatures (at least superficially) above that of the melting point of titania. The hardness ( $H$ ), elastic modulus ( $E$ ), and elasticity index ( $H/E$  ratio) on the cross section and top surface of these HVOF-sprayed titania coatings were evaluated using the Knoop technique and Vickers hardness measurements. The distribution of elastic modulus and hardness values was analyzed via Weibull statistics. The coating microstructure and phase composition were evaluated using scanning electron microscopy (SEM) and x-ray diffraction (XRD) analysis, respectively. The porosity level was determined via image analysis. It was observed that the coatings were uniform and very dense, consisting of rutile as the major phase. The optimized spray conditions allowed the production of thick coatings ( $\sim 740 \mu\text{m}$ ), which were shown to be in a state of residual compressive stress using Almen strip measurements.

**Keywords** HVOF, indentation, tailoring of microstructures, titania, Weibull modulus

## 1. Introduction

Thermal spray processing of pure ceramics via high velocity oxygen fuel (HVOF) is a relatively unexplored field. The low flame temperatures of the HVOF process and ceramic characteristics such as a high melting point, lack of plasticity, and low thermal conductivity impede coating formation. Despite these characteristics, early work<sup>[1]</sup> has shown that when these barriers are overcome, HVOF-sprayed titania coatings exhibit both high microstructural uniformity in the cross section and top surface and have very uniform mechanical properties. Weibull modulus values from hardness measurements are significantly higher than those of other air and vacuum plasma-sprayed ceramic coatings and HVOF-sprayed cermets.<sup>[1]</sup>

As already mentioned, the combination of the characteristics of the HVOF process with those of ceramic materials limits the usefulness of the HVOF technique for producing ceramic coatings. For those ceramic materials where it is used, the process window, or latitude in spray parameter settings, is normally quite tight. Currently, in-flight particle characteristics of thermal spray jets, such as temperature and velocity, can be monitored with specific diagnostic equipment, and their effects can be related to the microstructural features of the coating.<sup>[2]</sup> It is believed that to maximize the deposition efficiency, conditions have to be identified that result in the highest average particle temperature being reached. It is this constraint that limits the usefulness of HVOF for depositing ceramics and makes the optimization process so critical.

Although there is a large body of papers on the microstructural characteristics, mechanical properties, and phenomenol-

ogy of mechanical behavior of plasma-sprayed ceramics and HVOF and plasma-sprayed cermets, little data is available in the literature on HVOF-sprayed pure ceramics coatings. This area appears to be relatively unexplored and may offer new possibilities for producing certain ceramic coatings.

Of the various advanced ceramics, titania has one of the lowest melting points ( $1855^\circ\text{C}$ ), together with a relatively high thermal conductivity ( $8.8 \text{ W/mK}$ ),<sup>[3,4]</sup> which makes it a “good candidate” for being deposited using HVOF. Insight gained from spraying this material by HVOF may help to establish guidelines on the HVOF spraying of ceramics.

The current work, which builds on earlier research on HVOF titania,<sup>[1]</sup> presents the results of a study aimed first at optimizing the HVOF spraying conditions for titania and, then, of analyzing the microstructure and phases present in the resulting coating. This work also aims at evaluating the mechanical behavior of the optimized HVOF titania coatings via indentation techniques and compares the behavior of these coatings with the previously HVOF-sprayed titania<sup>[1]</sup> and those of other ceramic and metallic coatings sprayed by different techniques.

## 2. Experimental

### 2.1 Thermal Spraying and Particle Diagnostics

A fused and crushed titania ( $\text{TiO}_2$ ) feedstock [Flomaster 22.8(99) F4, F.J. Brodmann & Co., Harvey, LA] with a nominal particle size range from  $5\text{--}20 \mu\text{m}$  was sprayed using a HVOF torch (DJ 2700-hybrid, Sulzer-Metco, Westbury, NY). To optimize the spray parameters, the following approach was taken. The particle temperature ( $T$ ), velocity ( $V$ ), and diameter in the spray jet were measured using a diagnostic tool (DPV2000, Tecnar Automation, Saint Bruno, QC, Canada) for different combinations of spray parameter settings. This diagnostic unit uses a system based on optical pyrometry and time-of-flight measurements to obtain information on the spray jet. Individual particles are detected in the jet to provide temperature, velocity, and particle diameter information.<sup>[2]</sup> Using this tool, data was acquired for each combination of spray parameters by measuring a total of

R.S. Lima and B.R. Marple, National Research Council of Canada, 75 De Mortagne Boulevard, Boucherville, QC J4B 6Y4, Canada. Contact e-mail: rogerio.lima@nrc-nrc.gc.ca.

at least 3000 particles for each parameter set, which counts for approximately 2 min of spraying time. The in-flight characteristics were determined at the centerline of the HVOF spray jet, where the particle flow density was the highest.

After a series of tests that involved changing the flows and ratios of oxygen, propylene, air cooling, carrier gas, and spray distance, the optimized set of spray parameters was considered the one that exhibited the highest average particle temperature without causing damage to the spray torch due to excessive heat of the flame. Therefore, the so-called optimized set corresponds to the “hottest condition” provided by the DJ2700-hybrid torch under safe operating conditions. Hotter conditions can be reached and were observed during this work; however, under these hotter conditions torch parts, such as injectors, O-rings, and hoses, are more severely degraded. The optimized set of spray parameters are listed in Table 1, together with the set of spray parameters used in earlier work by the current authors.<sup>[1]</sup> The in-flight particle data (particle  $T$ ,  $V$ , and diameter) presented and discussed in this work were acquired at a spray distance of 20 cm (Table 1).

The coatings were deposited on low carbon steel substrates (length, 7.62 cm; width, 2.54 mm; thickness, 1.27 cm) that had been grit-blasted to roughen the surface before spraying. During the spraying process a cooling system consisting of air jets was applied to reduce coating temperature. The coating temperature was monitored during spraying using an optical pyrometer. The maximum coating temperature during the process was  $\sim 325$  °C. Coating thicknesses up to  $\sim 740$   $\mu\text{m}$  (29 mils) were attained.

To obtain some qualitative information on the residual stress condition of the coatings, an Almen strip (type, N; grade, I) (Electronics Inc., Mishawaka, IN) was mounted alongside the substrates and coated during the spraying process. The deflection of the Almen strip was read via an Almen gage (Model TSP-3, Electronics Inc., Mishawaka, IN) before and after the coating deposition. The difference between these two values indicated whether the coating was in compression (negative value) or tension (positive value). This Almen procedure was based on a technique described by Sauer and Sahoo.<sup>[5]</sup>

The value of deposition efficiency (DE) was also measured by depositing on a grit-blasted low carbon steel substrate of known dimensions using a predetermined powder feed rate, torch speed, and total number of passes, and then comparing the weight of the substrate before and after the deposition with respect to the feedstock feed rate.

**Table 1 HVOF Spray Parameters for Titania (DJ2700-Hybrid)**

Parameter	Optimized Set	Previous Set <sup>[1]</sup>
Propylene flow	176 scfh (83.1 slpm)	132 scfh (62.3 slpm)
Oxygen flow	664 scfh (313.4 slpm)	491 scfh (231.8 slpm)
Air flow	714 scfh (337 slpm)	786 scfh (371 slpm)
Carrier gas (N <sub>2</sub> ) flow	30 scfh (14.2 slpm)	20 scfh (9.4 slpm)
Powder feed rate	25 g/min	30–35 g/min
Spray distance	20 cm	20 cm
Feedstock	Flomaster 22.8 (99) F4	Amperit 782.0
	Fused and crushed ( $-20/+5$ $\mu\text{m}$ )	Fused and crushed ( $-22/+5$ $\mu\text{m}$ )

slpm, standard liters per minute; scfh, standard cubic feet per hour

## 2.2 Characterization

Samples of both the cross section and top surface of the titania coatings were vacuum-impregnated with a low viscosity epoxy and polished for study using scanning electron microscopy (SEM). Coating porosity was evaluated on the cross section of the coating using SEM and image analysis. A total of five SEM pictures were analyzed for porosity measurements.

X-ray diffraction (XRD) (Cu K $\alpha$  radiation) was used to determine the phases present in the feedstock and coating. A  $2\theta$  diffraction angle ranging from 20–80° (using a step size of 0.05° and step time of 2.5 s) was used. The particle size distribution of the feedstock was determined using a laser diffraction particle size analyzer (Beckman Coulter LS 13320, Beckman Coulter, Miami, FL).

## 2.3 Mechanical Properties and Treatment of Data

Vickers hardness measurements were performed under a 300 g load for 15 s on the cross section and top surface of the coatings. The elastic modulus was determined via a Knoop indentation technique<sup>[6,7]</sup> on the cross section and top surface of the coating under a load of 1000 g and indentation time of 15 s. For the cross sections, the indentations were applied near the centerline of the coating thickness, whereas for the top surface the indentations were randomly positioned (avoiding the edges). A total of 20 measurements were performed for each indentation series. This approach for determining elastic modulus was developed by Marshall et al.<sup>[6]</sup> based on the measurement of the elastic recovery of the in-surface dimensions of Knoop indentations. The ratio of the major ( $a$ ) to minor ( $b$ ) diagonals of the Knoop indenter is 7.11. During unloading, the elastic recovery reduces the length of the minor diagonal of the indentation impression ( $b'$ ), while the length of the major diagonal of the indentation impression ( $a'$ ) remains relatively unaffected. The difference between the known major to minor diagonal ratio (7.11) is compared with that of the indentation impression. The extent of recovery depends on the plasticity index or hardness-to-modulus ratio. The formula for determining elastic modulus ( $E$ , in Pa) is<sup>[6]</sup>:

$$E = \frac{(-\alpha H)}{\frac{b'}{b} - \frac{a'}{a}} \quad (\text{Eq 1})$$

where  $\alpha$  is a constant (0.45),  $H$  is Knoop hardness (in Pa),  $a'$  and  $b'$  are respectively the lengths of the major and minor diagonals of the indentation impression, and  $b/a$  is 1/7.11. One important point must be clarified regarding the measurements in the current study. When determining the elastic modulus of the cross section, the major diagonal of the Knoop indenter was positioned perpendicular to the substrate surface. As the measurement of the elastic modulus is strongly based on the minor diagonal, the elastic modulus results obtained for the cross section in this work represent the values parallel to the coating surface.

## 3. Results and Discussion

### 3.1 In-Flight Particle Characteristics

Figure 1 shows the histogram of particle temperature for the optimized and previous<sup>[1]</sup> set of spray parameters for HVOF ti-

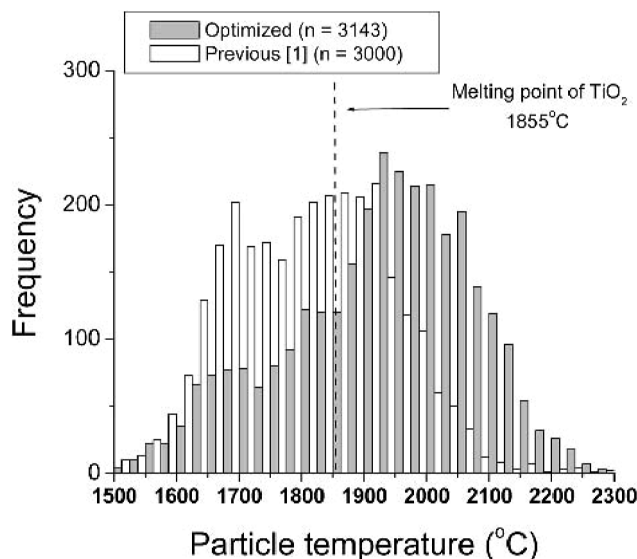


**Fig. 1** Histogram of particle temperature for the optimized and previous<sup>[1]</sup> spray parameters for HVOF titania

tania. The in-flight particle data were acquired at a spray distance of 20 cm (Table 1), the distance at which the substrate would normally be positioned when depositing a coating. The optimized value of average particle temperature is  $1925 \pm 163$  °C. This temperature is 70 °C above the melting point of titania, which has been reported to be 1855 °C.<sup>[8]</sup> This result is a significant improvement from that obtained for the previous set,<sup>[1]</sup> where the average particle temperature ( $1807 \pm 134$  °C) was 48 °C below the melting point of titania. It must be pointed out that, as with the majority of pyrometric measurements, errors related to calibration may be present in the particle temperature measurements; that is, the real particle temperature values may be higher or lower than those measured. However, according to Touloukian et al.,<sup>[9]</sup> at 1067 °C the emissivity values of the titania at the wavelengths of  $\sim 0.8$  to  $\sim 1.0$   $\mu\text{m}$  are very similar:  $\sim 0.92$  and  $\sim 0.93$ , respectively. The DPV2000 registers and analyzes infrared (IR) wavelengths at 0.787 and 0.995  $\mu\text{m}$ , respectively, and it is calibrated to give accurate temperature values on gray bodies, which have a constant emissivity in different wavelengths. Therefore, because the emissivity values of titania are similar at the two wavelengths analyzed by the DPV2000, it is thought that the values of particle temperature obtained during this work are a fair representation of the particle condition. It is important to point out that the particle temperature values obtained via pyrometric measurements represent surface temperature values; that is, the inner part of the particles may have lower temperatures.

Concerning particle velocity, the average velocity for the optimized parameter set is  $663 \pm 174$  m/s; that is, 13% higher than that of the previous one ( $588 \pm 124$  m/s).<sup>[1]</sup> Note that the kinetic energy increases as the square of the velocity, so that an increase of 13% may constitute an important gain.

Figure 2 shows a graph of particle temperature versus particle diameter for the optimized set of spray parameters. This graph reveals that the majority of the sprayed particles reached, at least superficially, the melting point of titania. Figure 2 is divided into

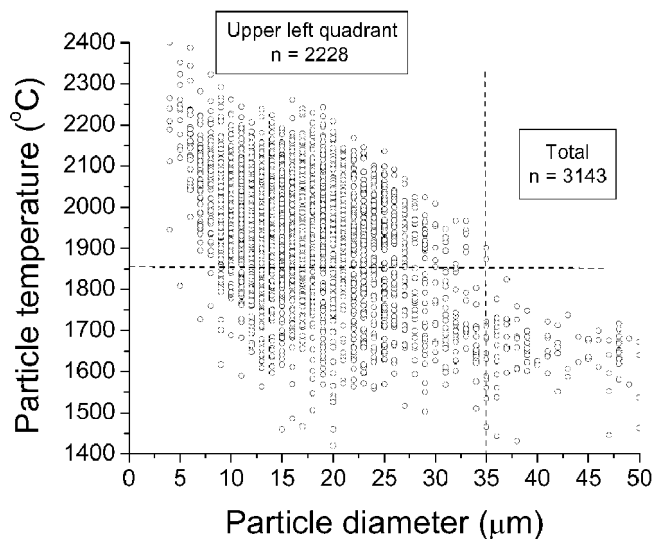


**Fig. 2** Plot of particle temperature versus particle diameter for the optimized set of spray parameters for HVOF titania

four quadrants by two dashed lines. The dashed line intersecting the particle temperature axis divides particles that have temperatures above and below 1855 °C (melting point of titania). The dashed line intersecting the particle diameter axis divides particles into those having diameters above or below 35  $\mu\text{m}$ . No particles larger than 35  $\mu\text{m}$  have temperatures higher than 1855 °C. Therefore, as assumed in the previous work,<sup>[1]</sup> the particles that are found in the upper left quadrant of Fig. 2 should play the major role in coating formation. They represent 71% of the total number of sprayed particles (44% of the total volume), whereas for the previous work a similar type plot showed that the particles situated in the upper left quadrant represented only 38% of the total number of particles (8% of the total volume). The results of DE reflect very well this characteristic. The DE for the optimized set of spray parameters is  $\sim 45\%$  while the DE for the previous work was  $\sim 30\%$ ; that is, there is a relative gain of 50% in DE when using the optimized set of spray parameters.

When analyzing the particles situated in the upper left quadrant of Fig. 2, it is observed that the average particle velocity is  $670 \pm 177$  m/s. The coefficient of variation (CV) in this data is 26%. There is not a significant difference between the value for the average velocity for particles in this quadrant and that for the overall particle velocity ( $663 \pm 174$  m/s) when all particles are considered. For the particles situated in the upper left quadrant (Fig. 2), the average particle temperature is  $2008 \pm 97$  °C with a CV of 5% for that data. This average particle temperature is 83 °C above the overall average particle temperature and 153 °C above the melting point of titania. When compared with the results obtained in the earlier study<sup>[1]</sup> this is a considerable gain, particularly when the temperature is in the critical region around the melting point. The average size of the particles situated in the upper left quadrant of Fig. 2 is  $15 \pm 6$   $\mu\text{m}$ . It is important to note that particles larger than 35  $\mu\text{m}$  exhibited temperatures below that of the melting point of titania. These characteristics show that a tight particle size is very important when spraying a typical advanced ceramic such as titania with the HVOF system. This is

**Table 2 Particle Size Distribution Determined via Laser Diffraction (Volume Statistics)**

Feedstock characteristics, TiO <sub>2</sub>	Flomaster 22.8(99)F4, Optimized Set	Amperit 782.0, Previous Set <sup>[1]</sup>
Average particle size (μm)	24	17
d <sub>10</sub> (μm)	8	8
d <sub>50</sub> (μm)	19	17
d <sub>90</sub> (μm)	46	28

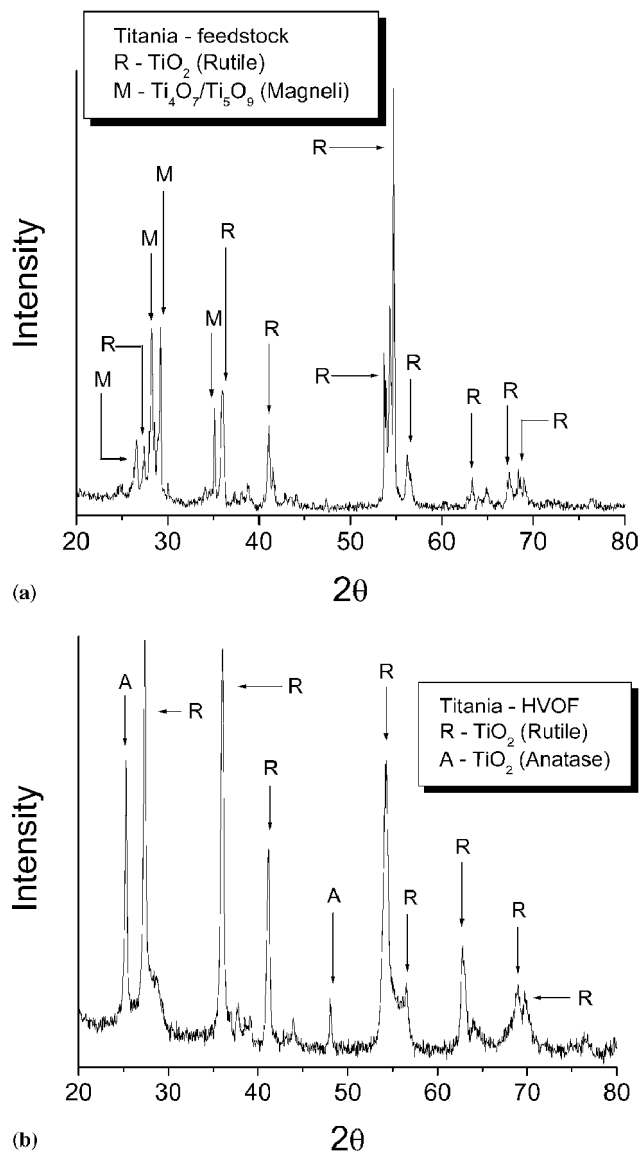
probably one of the reasons why the CV of average particle temperature in the upper left quadrant presented the low value of 5%. It is also thought that particle density may be an important factor when spraying ceramics via HVOF. In this work, fused and crushed (dense) particles were used as the feedstock. Porous particles (e.g., agglomerated), due to the lower thermal conductivity, may require more energy to be sprayed than that required by dense feedstock particles.

Table 2 shows the results of particle size distribution (in volume) of the feedstock determined via laser scattering. The d<sub>90</sub> of the titania “Flomaster 22.8(99)F4” was 46 μm. Although this feedstock has a nominal particle size distribution varying from 5–20 μm, larger particles are present as a probable result of imperfect particle sieving. According to the DPV2000, the overall average particle size in the spray jet was 18 ± 10 μm; the d<sub>50</sub> and average particle size of the feedstock determined via laser scattering (Table 2) were 19 and 24 μm, respectively. The particle size distribution of the titania feedstock “Amperit 782.0” used in the previous work<sup>[1]</sup> was also analyzed (Table 2). It has a similar particle size distribution (average, d<sub>10</sub> and d<sub>50</sub>) to that of the titania Flomaster 22.8(99)F4, but it exhibits a lower upper cut (d<sub>90</sub>).

### 3.2 Crystallographic Phases

Figure 3 shows the XRD patterns of the titania feedstock and the HVOF coating. The spectrum shown in Fig. 3(a) indicates that the process used in producing the titania feedstock resulted in the presence of rutile, anatase, and Magnéli phases (Ti<sub>n</sub>O<sub>2n-1</sub>; n = 4 to 10). After HVOF spraying, the coating (Fig. 3b) contained rutile and anatase as the major and minor phases, respectively. It is assumed that the thermodynamic conditions during the spray process transformed most of the Magnéli phases of the feedstock into rutile or anatase. No significant degradation of the titania phase was observed; that is, the HVOF coating contained the stoichiometric TiO<sub>2</sub> phase.

The Magnéli phases are formed when TiO<sub>2</sub> is annealed in a reducing atmosphere.<sup>[8]</sup> It is important to notice that the overall average particle temperature of the HVOF-sprayed titania particles, even with the optimized parameters, is just 70 °C above the melting point of titania (Fig. 1). As a consequence, it is quite possible that the majority of the titania particles do not fully melt during the HVOF process. Therefore, no significant changes in the TiO<sub>2</sub> coating stoichiometry were noticed during this and previous work.<sup>[1]</sup> Buchmann and Gadov<sup>[10]</sup> speculate that the HVOF process may have an oxidizing effect on titania, thereby impeding the loss of oxygen that can lead to the formation of the Magnéli phases.

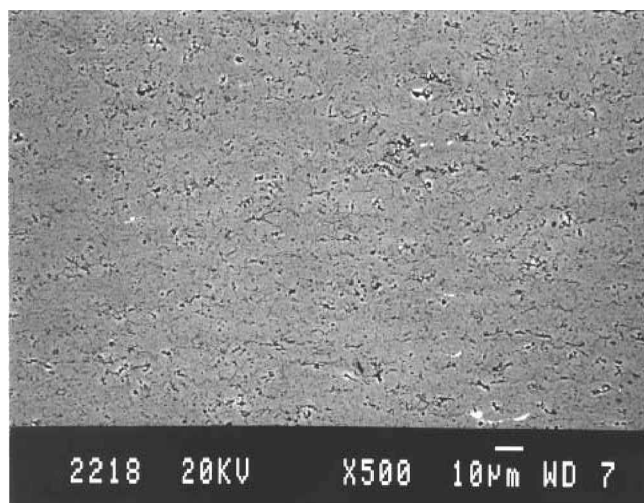


**Fig. 3** (a) XRD pattern of the titania feedstock [Flomaster 22.8(99)F4]; (b) XRD pattern of the optimized HVOF titania coating

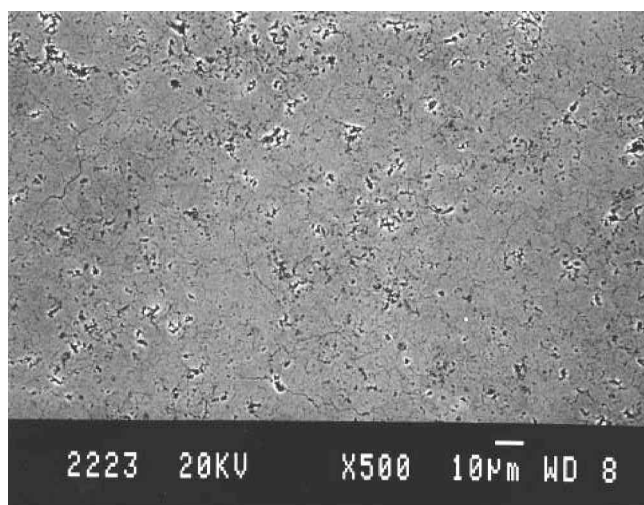
### 3.3 Coating Microstructure, Porosity, and Residual Stress

Figure 4 shows SEM pictures of the coating microstructure for the cross section and top surface. The coating has very low porosity levels (<1%). It is thought that the high impact velocity of the sprayed particles is one of the main factors producing this low porosity level. The average particle velocity was 663 ± 174 m/s. The microstructures are dense and homogeneous. Due to these characteristics, it is believed that these coatings should have a tendency to exhibit a near isotropic behavior in their properties.<sup>[1]</sup> Results to be presented in the following sections will show that this is, in fact, the case.

The results of Almen strip measurements (resulting deflection, −196 μm) indicate that the HVOF titania coatings are under a residual compressive stress. This is probably one of the reasons



(a)



(b)

**Fig. 4** (a) Cross-section of the optimized HVOF titania coating; (b) top surface of the optimized HVOF titania coating

why thick ( $\sim 740 \mu\text{m}$ ) and dense coatings were produced without spalling from the substrate.

### 3.4 Hardness, Elastic Modulus, and Weibull Modulus

Figure 5 shows the Vickers hardness numbers (300 g load) for the cross section and top surface of two sets of HVOF titania coatings: one deposited in this study using so-called optimized spray conditions and a second produced in an earlier study.<sup>[1]</sup> The results show that the hardness on the cross section of the optimized coating ( $\text{HV} = 879 \pm 49$ ) has a value similar to that of the coating produced in the earlier work ( $\text{HV} = 832 \pm 42$ ),<sup>[1]</sup> whereas the top surface hardness value of the optimized coating ( $\text{HV} = 951 \pm 43$ ) is significantly higher than that of the previous one ( $\text{HV} = 806 \pm 42$ ). The coating thicknesses for the optimized and previous work<sup>[1]</sup> were  $\sim 740$  and  $\sim 340 \mu\text{m}$ , respectively. Despite the difference in coating thickness, the maximum coating

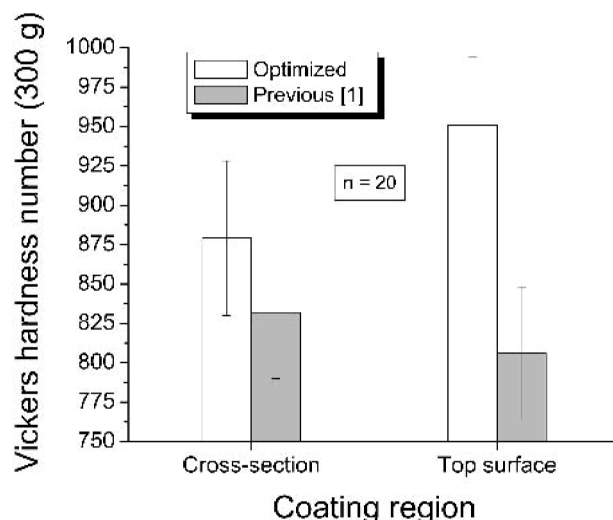


**Fig. 5** Vickers hardness number for the optimized and previous<sup>[1]</sup> HVOF titania coatings on the cross section and top surface

temperature was kept the same for both types of coatings during the deposition (i.e.,  $\sim 325^\circ\text{C}$ ). This homogeneity in coating temperature should provide uniformity in coating microstructure.

The Weibull modulus values from Vickers hardness of these coatings are compared in Fig. 6. The Weibull modulus values on the cross section of the optimized coatings and those produced in the earlier study are 19 and 20, respectively. The top surface Weibull modulus values for the optimized and previous coating are 23 and 20, respectively. It is noticed that the Weibull modulus values for the cross sections for these two coatings are similar while the Weibull modulus value of the top surface for the optimized coating exhibits an improvement over that found in the previous study. In earlier work,<sup>[1]</sup> a comparison was made between the Weibull modulus from Vickers hardness values of HVOF titania and several ceramic thermal spray coatings sprayed with different processes by different groups of researchers. Weibull modulus values ranging from 19–23, as obtained during this work, are significantly higher than the majority of Weibull modulus values determined for other ceramic thermal spray coatings.<sup>[1]</sup> It is important to point out that the Weibull modulus is a measure of the variability of a material's mechanical properties.<sup>[11]</sup> Two or more materials with similar mechanical property values (i.e., average and standard deviation) may be differentiated and compared through their respective Weibull modulus values. The Weibull modulus may be used to determine which material has higher uniformity and reliability. It is important to note that a high value of Weibull modulus does not imply a high mechanical property value. The Weibull modulus indicates the degree of uniformity of a mechanical property throughout the sample, not its absolute value.

In earlier work,<sup>[1]</sup> it was suggested that a combination of three conditions contributes to producing coatings having high Weibull modulus of hardness: (1) phase uniformity of the coating, (2) microstructural uniformity within the coating and high density, and (3) narrow particle size range of the feedstock, resulting in a uniform particle heating. When analyzing the experimental results presented in the previous sections, it is noticed that these three conditions are found. Therefore, these results

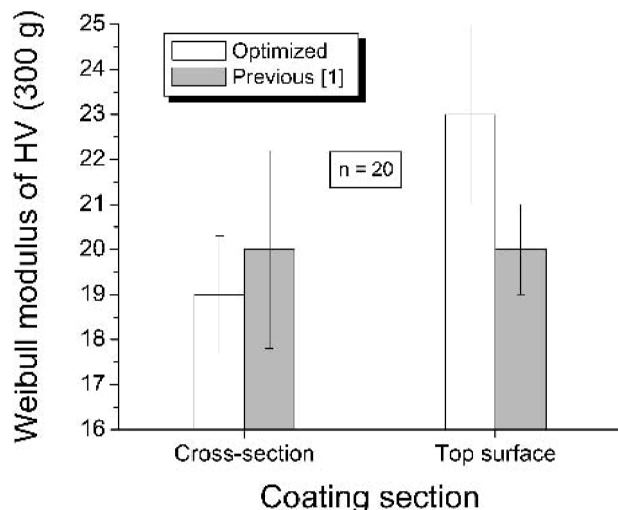


**Fig. 6** Weibull modulus values from Vickers hardness number for the optimized and previous<sup>[1]</sup> HVOF titania coatings on the cross section and top surface

reinforce the claim that if the intent is to engineer a highly uniform thermal spray coating, an important part of the process should focus on satisfying these three conditions.

The various mechanical properties of a material are often related. Hardness measurements via indentation techniques explore the interaction between splats, splat boundaries, semimolten particles, phases, morphology, cracks, pores, and grains. As a consequence, it is not unreasonable to suggest that other coating mechanical properties (e.g., elastic modulus and fracture toughness) also influenced by these interactions may correlate with the “hardness behavior”; that is, a high Weibull modulus of hardness should indicate a low variability of other mechanical properties (and vice-versa) originating from the same material interactions as that of the hardness. Mechanical properties such as elastic modulus<sup>[6,7]</sup> and fracture toughness<sup>[12]</sup> can also be measured via indentation techniques and their results analyzed via a Weibull distribution.

The elastic modulus of the optimized HVOF titania coating was measured via the Knoop indentation technique.<sup>[6,7]</sup> The Knoop hardness numbers for the cross section and top surface are  $833 \pm 16$  and  $812 \pm 17$ , respectively. Figure 7 shows the Weibull modulus values of Knoop hardness and elastic modulus of the optimized HVOF titania coatings, soda lime “window” glass (bulk), together with values from the literature for several other ceramic coatings, all obtained at an indentation load of 1000 g.<sup>[7]</sup> When comparing Weibull modulus of indentation measurements of two or more materials, it is imperative to do the comparison using the same indentation load<sup>[1]</sup> due to the load dependence of Weibull modulus values originating from indentation techniques. As expected, due to the characteristics of these coatings (the three conditions discussed earlier), the Weibull modulus values of Knoop hardness of the optimized HVOF titania are far superior to those of other ceramic coatings. The relatively high thermal conductivity of titania ( $8.8 \text{ W/mK}$ )<sup>[3,4]</sup> should also aid in a uniform heating of the titania-sprayed particles (condition no. 3).

The elastic modulus values for the cross section and top sur-

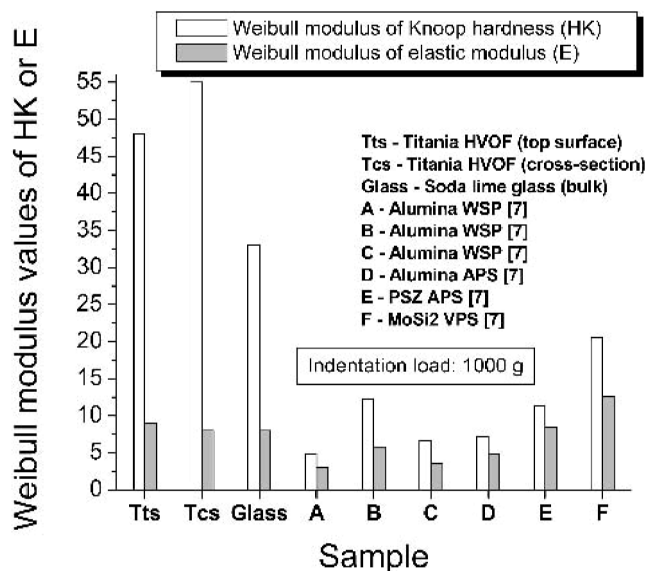


**Fig. 7** A comparison of Weibull modulus values of Knoop hardness number and elastic modulus for the optimized HVOF titania coatings, soda lime glass (bulk), and various as-sprayed thermal spray ceramic coatings (data from the literature) for the indentation load of 1000 g. Weibull modulus values of the references were taken from the cross section. For all coatings, the major diagonal was oriented perpendicular to the coating surface.

face of the HVOF titania coating were found to be  $146 \pm 18$  and  $134 \pm 16$  GPa, respectively. From the literature, the elastic modulus of bulk titania (rutile) is known to be 282 GPa.<sup>[8]</sup> Therefore, the elastic modulus of this coating is ~50% of that of the bulk. This lies at the upper limit of the range for the elastic modulus of thermal spray coatings that, according to Pawlowski,<sup>[13]</sup> is in-between 20% and 50% of that of the bulk.

The origin of the lower elastic modulus values in thermal spray coatings as compared with those for the bulk material has been discussed and explained by McPherson.<sup>[14-16]</sup> The mechanical behavior of a thermal spray coating is limited by the degree of contact between splats within the coating or between the splats and substrate. The limited “true contact area” between splats arises due to air entrapment and thermal stresses that occur during the spraying process and is an inherent coating characteristic. The high particle velocities of the HVOF systems may improve the “true contact area,” thereby increasing the values of mechanical properties and coating uniformity. The high coating density and very low porosity values (<1% as determined by image analysis) of the optimized HVOF titania coatings produced in this work are consistent with this explanation. The high values of elastic modulus of the HVOF titania are then explained.

Figure 7 also shows the Weibull modulus values of elastic modulus for the optimized HVOF titania, soda lime glass (bulk), and several other as-sprayed ceramic thermal spray coatings taken from the literature.<sup>[7]</sup> The HVOF titania exhibits Weibull modulus values higher or similar to those of most other ceramic coatings. The exception is the vacuum plasma spray (VPS) MoSi<sub>2</sub> coating, which exhibits the highest value. It is speculated that this arises because VPS coatings are generally very dense,<sup>[13]</sup> which contributes to a high coating uniformity (one of

the three conditions identified earlier as playing an important role in obtaining high Weibull modulus values).

It is noticed that the Weibull modulus values of the Knoop hardness of the HVOF titania coatings are much higher than those of other ceramic coatings (Fig. 7). Unfortunately, the present authors have not found in the literature the Weibull modulus value of Knoop hardness (at 1000 g load) of bulk titania. This value would have been very important to compare and classify the microstructural homogeneity of these HVOF titania coatings. Nonetheless, the elastic modulus of an ordinary soda lime “window” glass (bulk) was measured via Knoop technique at 1000 g load ( $E = 64 \pm 7$  GPa;  $HK = 473 \pm 13$ ). The Weibull modulus values of the soda lime glass for the Knoop hardness and elastic modulus are 33 and 8, respectively (Fig. 7). The Weibull modulus of Knoop hardness for the glass is still lower than that presented by the HVOF titania (~50); however, it is significantly higher than those of other ceramic coatings (Fig. 7). It is thought that if the Weibull modulus value of Knoop hardness of an ordinary window glass is 33, the Weibull modulus value of a pure, dense, and uniform advanced ceramic (bulk), such as titania, should reach higher values. And these bulk values may be at the same or at higher level than those of the HVOF titania, and then they would explain or clarify the high Weibull modulus of Knoop hardness observed for these HVOF titania coatings.

### 3.5 Elasticity Index and Coating Isotropy

When an indenter is loaded into a flat surface of a test specimen, it leaves a residual indentation impression. Hardness is then measured by dividing the indentation load by the projected area of the indentation impression or by the penetration depth of the indenter, depending on the technique being used. It is clear that hardness is an indicator of the irreversible or plastic deformation behavior of the test material. But it must be remembered that the final dimensions of the indentation impression also depend to some extent on the reversible deformation or recovery, which is also a material behavior characteristic.<sup>[6,7,17]</sup> Therefore, one can argue that indentation measurements are an elastic-plastic parameter.

The elastic recovery during unloading of an indenter can exhibit a wide range of behaviors. Extremes in depth recovery are shown by “soft” metals where recovery is negligible, and by “highly elastic” rubbers where recovery is nearly complete. Typically, brittle materials such as ceramics will exhibit a behavior between the two extremes. Lawn and Howes<sup>[17]</sup> quantified the indentation recovery in terms of well-defined elastic-plastic parameters. The extent of the recovery depends on the hardness-to-elastic modulus ratio (i.e.,  $H/E$ ). The  $H/E$  ratio, also known as elasticity index, is an indicator of a material’s capacity to absorb or dissipate energy. High  $H/E$  values will be found in highly elastic materials, whereas low  $H/E$  values will be found in more plastic materials. The elasticity index is an important parameter of the coating microstructure and it has not been extensively explored in the thermal spray field. It can be investigated when one determines the elastic modulus via Knoop indentations.<sup>[6,7,18]</sup> As a consequence, analyzing the behavior of the  $H/E$  ratio on the cross section and top surface may constitute an important way to analyze and understand the mechanical behavior

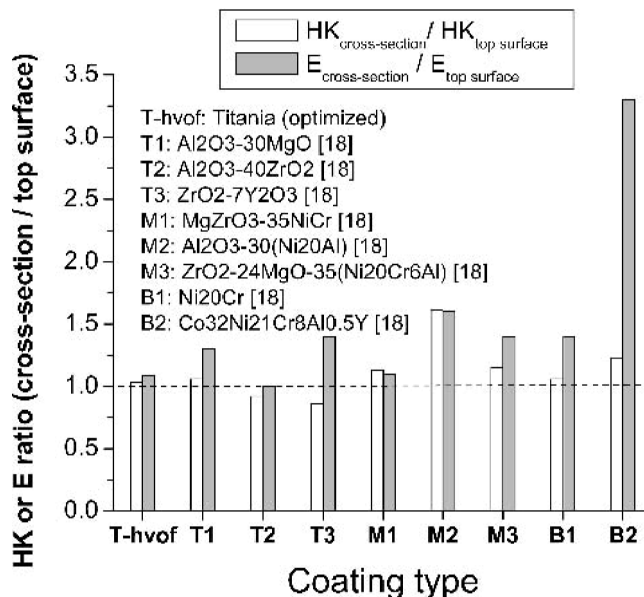


**Fig. 8** A comparison of Knoop hardness (HK) and elastic modulus (E) ratio (cross section/top surface) for the optimized HVOF titania coatings and several APS coatings (data from the literature). For all coatings, on the cross section, the major diagonal was oriented perpendicular to the coating surface.

of these types of coatings, and it may be an important parameter for future modeling of thermal spray coatings.

Figure 8 shows the results for the Knoop hardness and elastic modulus ratios for the optimized HVOF titania and several APS (air plasma spray) coatings. It can be seen that the optimized HVOF titania coating is, on average, more isotropic than the other APS coatings; that is, its both ratios ( $HK_{cs}/HK_{ts}$  and  $E_{cs}/E_{ts}$ ) are close to 1.0. This behavior has been reported earlier<sup>[11]</sup> for Vickers hardness when comparing the previous HVOF titania coatings with other results in the literature. It was concluded that the HVOF titania coatings, due to a high density, behave nearly as the bulk material. And it is thought that this “near isotropic behavior” should also be observed for other very dense coatings.

Figure 9 shows the elasticity index ( $H/E$  ratio) of the cross section and top surface for the optimized HVOF titania coatings and several APS coatings. The  $H/E$  ratio for the cross section and top surface are 0.0562 and 0.0597, respectively. As observed in the results of Knoop hardness and elastic modulus (Fig. 8), the HVOF titania is among the most uniform coatings discussed in this paper; that is, its values of elasticity index are near isotropic (Fig. 9). Nonetheless, one important observation can be made. For all these coatings, the  $H/E$  ratio is slightly or significantly higher in top surface than it is in the cross section. Thus, apparently, thermal spray coatings tend to behave more elastically in the top surface and more plastically in the cross section.

However, when carefully analyzing Fig. 8, it is observed that the majority of the Knoop hardness values of the cross section are slightly or significantly higher than those of the top surface; that is, the ratio of cross section to top surface hardness is generally higher than 1.0. Apparently, there is a paradox. The microstructure of the cross section has a “more plastic behavior” (lower  $H/E$  ratio) than that of the top surface, but the hardness

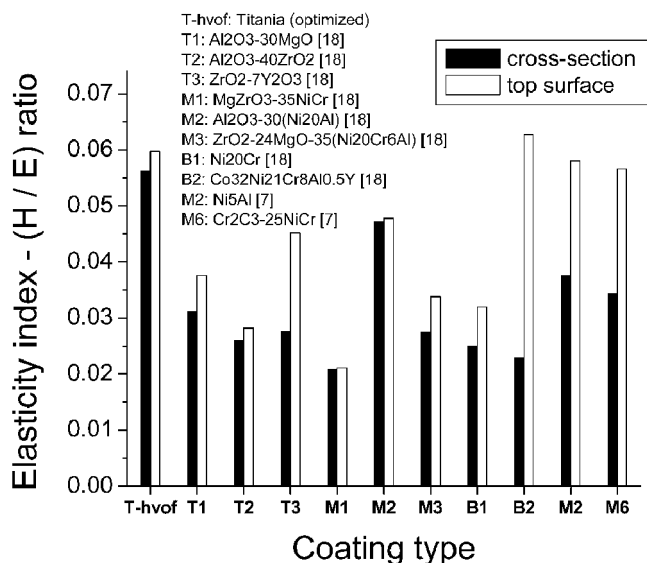


**Fig. 9** A comparison of elasticity indexes ( $H/E$  ratio) of the cross section and top surface for the optimized HVOF titania coatings and several APS coatings (data from the literature). For all coatings, on the cross section, the major diagonal was oriented perpendicular to the coating surface.

values of the cross sections are generally higher than those of the top surface.

To understand this “apparent paradox,” one may imagine the microstructure of a thermal spray coating as a “pile of splats” having pores of approximately ellipsoidal shape, where the major axis of the ellipsoid is parallel to the spread plane of the splats. Leigh et al.<sup>[7]</sup> analyzed this structure and postulated that due to the pore geometry, when one analyzes the coating from the cross section, the “relative porosity” is lower than that when the coating microstructure is analyzed from the top surface. Due to this pore shape anisotropy, and knowing that porosity reduces elastic modulus<sup>[19,20]</sup> and hardness values,<sup>[21]</sup> it is possible to understand the origin of the higher values of hardness on the cross section compared with the top surface. The elastic modulus (and hardness as a correlated property) is related not only to the total porosity, but also to the pore morphology.<sup>[22]</sup>

The explanation provided by Leigh et al.<sup>[7]</sup> explains the higher cross-sectional values of hardness generally found in thermal spray coatings. However, to understand the factors that give rise to a greater degree of plastic behavior in the cross section is more complex. One must remember that during the cross-section measurements, the major diagonal was placed perpendicular to the coating surface. Under this indentation geometry, the minor diagonal is then parallel to the spread direction of the splats. As a direct consequence, when indenting a coating on the cross section, the minor diagonal of the tip of the Knoop indenter contacts and forces the coating microstructure at its weakest point, the intersplat interface, as postulated by McPherson.<sup>[14–16]</sup>

As a consequence of the anisotropic microstructure of the thermal spray coatings, when indenting on the cross section with the major diagonal perpendicular to the coating surface, the minor diagonal cleaves the weak interface between splats.<sup>[14–16]</sup> Therefore, the minor diagonal of the indenter encounters less resistance to penetration and yielding, thus minimizing the re-

covery behavior. At the same time, the major diagonal contacts the zone of “lower relative porosity,” which reflects in higher hardness values.<sup>[7]</sup> Thus, the coating tends to be more compliant in the cross section although being harder. Probably, this is a typical and unique characteristic of thermal spray coatings.

Another factor may be considered regarding this apparent paradox. When analyzing the coating cross section, the major and minor diagonals of the Knoop indenter have very different interactions with the coating microstructure. But when analyzing the coating top surface, the major and minor diagonals of the Knoop indenter do not have any special orientation or preferential interaction with respect to the coating microstructure. Both indenters probe and measure the same structure. Therefore, Knoop indentation impressions on the cross section are naturally anisotropic, whereas in the top surface they have an isotropic character. Thus, depending on the desired application or objectives, it is important to determine whether measurements on the cross section or top surface will provide the more relevant information.

### 3.6 Final Considerations

When observing Fig. 5, it is noticed that the Vickers hardness values of the optimized HVOF titania coatings are higher than those of the previous work.<sup>[11]</sup> There is a slight increase in hardness in the cross section and a significant increase in hardness in the top surface. Regarding the Weibull modulus of Vickers hardness (Fig. 6), the values of the cross section are relatively similar, whereas for the top surface there is a significant increase of the Weibull modulus for the optimized HVOF titania. Nonetheless, the gains in Vickers hardness and Weibull modulus were insignificant when compared with the gain in DE. When changing from the previous to the optimized set of parameters, there was a relative gain of 50% in DE.

Analysis of the plot of particle temperature versus particle diameter (Fig. 2) indicates that the particles situated in the upper left quadrant represent 71% of the total number of particles (44% of the total volume). As previously discussed, it is thought that the particles situated in the upper left quadrant are the main contributors to the coating formation. The same type of plot was used in the previous work,<sup>[11]</sup> and in that study the particles situated in the upper left quadrant represented 38% of the overall number of particles (8% of the total volume). Figure 1 shows the histograms of particle temperature for the optimized and previous<sup>[11]</sup> HVOF titania. It is noticed that the frequency of particles situated above the melting point of titania is significantly higher for the optimized parameters. These observations (Fig. 1 and 2) explain the DE gain from the previous to the current work. However, the significant DE gain does not translate into a similar, or even significant, gain in the mechanical properties values; that is, for this case there is no apparent correlation between DE and mechanical properties.

Analyzing the upper left quadrant of Fig. 2 shows that the CV of particle temperature is 5%, whereas for the previous work it was 4%. In both cases the particles had similar average velocities. Thus, this very uniform particle heating, even with the different spray parameters used, is probably the result of the narrow particle size distribution of both titania feedstocks (Table 2). This uniform heating is reflected in the “relative uniformity” of Vickers hardness and Weibull modulus of the optimized and



previous HVOF titania coatings. The significant percentage difference of particles above the melting point of titania (upper left quadrant) is reflected in the significant DE gain obtained from the previous to the current work.

Therefore, it is thought that when one seeks to increase the robustness of the process with regard to the spray parameter process window for a given feedstock, it is necessary to work with feedstocks having a narrow particle size distribution. Results from the current and previous<sup>[11]</sup> studies appear to indicate that even if a feedstock with a narrow particle size distribution is sprayed using “nonoptimized parameters,” the quality of the coating will be similar to that sprayed using the “optimized parameters.” Although there may be a significant decrease in DE when nonoptimized parameters are used, the mechanical properties should not significantly be affected. To summarize, feedstocks having a narrow particle size distribution tend to enlarge the thermal spray process window within which acceptable coatings can be produced.

#### 4. Conclusions

- The optimized titania coatings produced using HVOF (DJ2700-hybrid) spraying exhibited high density, low porosity, and a uniform microstructure in the cross section and top surface. A deposition efficiency of 45% could be achieved using the optimized conditions.
- At the centerline and spray distance of 20 cm, 71% of the total number of sprayed particles (44% of the total volume) exhibited temperatures above (at least superficially) the melting point of titania. The average particle impact velocity was  $663 \pm 174$  m/s.
- The coatings are under residual compressive stress. Thick coatings ( $\sim 740$   $\mu\text{m}$ ) were achieved without spalling.
- The optimized HVOF titania coatings contained rutile as the major phase and minor amounts of anatase. No significant degradation was observed in the  $\text{TiO}_2$  stoichiometry. This probably results from the partial particle melting, low temperature of the HVOF system, and the oxidizing effect of the oxygen present in the HVOF flame.
- Small particle sizes and a narrow particle size distribution (e.g., from 5 to 20  $\mu\text{m}$ ) are very important characteristics when spraying ceramics, such as titania, via HVOF DJ2700-hybrid. Dense particles, due to a higher thermal conductivity, may also be an important characteristic.
- The HVOF titania coatings exhibited a near isotropic behavior (cross section and top surface) with respect to Vickers and Knoop hardness, elastic modulus, and elasticity index. The origin of this isotropy is probably related to the high coating density and uniformity provided by the HVOF system.
- The HVOF titania coatings exhibited higher Weibull modulus of both hardness and elastic modulus when compared with the majority of other as-sprayed ceramic/cermet thermal spray coatings reported in the literature and tested with the same indentation load and indenter diagonal orientation with respect to coating microstructure. The origin of this high uniformity (high Weibull modulus values) lies in the (1) phase uniformity, (2) microstructural uniformity and

high density, and (3) narrow particle size range of the feedstock, resulting in a uniform particle heating.

- For the type and characteristics of feedstock used, the spray parameter process window must be quite narrow for high DE to be achieved. However, coating uniformity and hardness are much less sensitive to changes in spray parameters. Feedstocks having a narrow particle size distribution tend to enlarge the process window in thermal spray.
- By comparing the results of this work with others from the literature, it is noticed that the coating hardness in the cross section tends to be higher than that of the top surface; however, the microstructure of the cross section tends to have a more plastic behavior (lower  $H/E$  ratio) than that of the top surface. The explanation for this apparent paradox is found in the position and orientation of the minor and major diagonals of the Knoop indenter with respect to coating microstructure. It is thought that when indenting on the cross section, the minor diagonal (which is mainly responsible for  $E$  measurements) “easily” cleaves the weak intersplat contacts, encounters less resistance to penetration and yielding, and minimizes the recovery behavior.

#### Acknowledgments

The authors want to thank Dr. J.F. Bisson for fruitful discussions on in-flight particle diagnostics and for his willingness and curiosity in discussing the microstructural characteristics of thermal spray coatings. The authors also want to thank F. Belval for HVOF spraying, M. Lamontagne for the DPV2000 measurements, E. Poirier for metallography, and M. Thibodeau for scanning electron microscopy. Special thanks are due to Bill Rusch and Michael Breitsamer from Sulzer-Metco, for information concerning the spray conditions and high temperature limits of the DJ2700-hybrid torch.

#### Appendix: Weibull Distribution

Each series of indentation results was fitted to a Weibull distribution.<sup>[23]</sup> According to Weibull theory, the probability that a sample will fail or yield at a particular strength or random value ( $x_i$ ) is  $P_i$ , given by Eq A.1:

$$P_i = 1 - \exp \left[ - \left( \frac{x_i - x_u}{x_0} \right)^m \right] \quad (\text{Eq A.1})$$

where  $x_u$  is the threshold stress below which there is no failure,  $x_0$  is the characteristic strength or value below which 63.2% of the data lie, and  $m$  is the Weibull modulus. This three-factor Weibull expression is actually rarely used because there does not seem to be a threshold stress for brittle materials and because it is mathematically inconvenient. A more practical form is the two-factor Weibull function:

$$P_i = 1 - \exp \left[ - \left( \frac{x_i}{x_0} \right)^m \right] \quad (\text{Eq A.2})$$

To fit a set of mechanical property data to the Weibull distribution, one first ranks the samples in order of increasing mechani-

cal property value and assigns an index:  $i = 1$  for the lowest value  $x_1$ ,  $i = 2$  for the second lowest value  $x_2$ , and so on, up to  $i = N$  for the highest value of mechanical property  $x_N$ . For each sample, an estimate for the probability of failure is assigned by  $P_i = i/(N + 1)$ .<sup>[24]</sup> The data is finally plotted in the following linearized form of the Weibull distribution:

$$\ln \left[ \ln \left( \frac{1}{(1 - P_i)} \right) \right] = m \ln(x_i) - m \ln(x_0) \quad (\text{Eq A.3})$$

The Weibull modulus  $m$  is determined from the slope of the  $\ln[\ln(1/(1 - P_i))]$  versus  $\ln x_i$  plot, and the characteristic value  $x_0$  comes from the intercept. These are often determined using the least-squares method. The above approach was used to determine the Weibull modulus for Vickers and Knoop hardness and the elastic modulus for the titania coatings.

## References

1. R.S. Lima and B.R. Marple: "High Weibull Modulus HVOF Titania Coatings," *J. Therm. Spray Technol.*, 2003, 12(2), pp. 240-49.
2. M. Prystay, P. Gougeon, and C. Moreau: "Structure of Plasma-Sprayed Zirconia Coatings Tailored by Controlling the Temperature and Velocity of the Sprayed Particles," *J. Therm. Spray Technol.*, 2001, 10(1), pp. 67-75.
3. MatWeb: The Online Materials Information Resource, <<http://www.matweb.com>>, 2002.
4. R.L. Lehman: "Overview of Ceramic Design and Process Engineering" in *Engineered Materials Handbook, Vol. 4: Ceramics and Glasses*, S.J. Schneider, ed., ASM International, Materials Park, OH, 1991, pp. 29-37.
5. J.P. Sauer and P. Sahoo: "HVOF Process Control Using Almen and Temperature Measurement" in *Thermal Spray 2001: New Surfaces for a New Millennium*, C.C. Berndt, K.A. Khor, and E.F. Lugscheider, ed., ASM International, Materials Park, OH, 2001, pp. 791-96.
6. D.B. Marshall, T. Noma, and A.G. Evans: "A Simple Method for Determining Elastic-Modulus-to-Hardness Ratio Using Knoop Indentation Measurements," *J. Am. Ceram. Soc.*, 1982, 65(10), C-175-C-176.
7. S.H. Leigh, C.K. Lin, and C.C. Berndt: "Elastic Response of Thermal Spray Deposits Under Indentation Tests," *J. Am. Ceram. Soc.*, 1997, 80(8), pp. 2093-99.
8. M. Miyayama, K. Koumoto, and H. Yanagida: "Engineering Properties of Single Oxides" in *Engineered Materials Handbook, Vol. 4: Ceramics and Glasses*, S.J. Schneider, ed., ASM International, Materials Park, OH, 1991, pp. 748-57.
9. Y.S. Touloukian, D.P. Witt, and R.S. Hertz: *Thermal Radiative Properties: Coatings—Thermophysical Properties of Matter*, Vol. 9, IP/ Plenum, New York-Washington, 1972.
10. M. Buchmann and R. Gadow: "Mechanical Characterization of APS and HVOF Sprayed TiO<sub>2</sub> Coatings on Light Metals" in *Thermal Spray 2001: New Surfaces for a New Millennium*, C.C. Berndt, K.A. Khor, and E.F. Lugscheider, ed., ASM International, Materials Park, OH, 2001, pp. 643-52.
11. T.H. Courtney: *Mechanical Behavior of Materials*, McGraw-Hill, New York, 1990.
12. G.N. Heintze and R. McPherson: "A Further Study of the Fracture Toughness of Plasma-Sprayed Zirconia Coatings," *Surf. Coat. Technol.*, 1988, 36, pp. 125-32.
13. L. Pawlowski: *The Science and Engineering of Plasma-Sprayed Coatings*, Wiley, West Sussex, UK, 1995.
14. R. McPherson: "A Review of Microstructure and Properties of Plasma Sprayed Ceramic Coatings," *Surf. Coat. Technol.*, 1989, 39/40, pp. 173-81.
15. R. McPherson: "The Relationship Between the Mechanism of Formation, Microstructure and Properties of Plasma-Sprayed Coatings," *Thin Solid Films*, 1981, 83, pp. 297-310.
16. R. McPherson and B.V. Shaffer: "Interlamellar Contact Within Plasma-Sprayed Coatings," *Thin Solid Films*, 1982, 97, pp. 201-04.
17. B.R. Lawn and V.R. Holmes: "Elastic Recovery at Hardness Indentations," *J. Mater. Sci.*, 1981, 16, pp. 2745-52.
18. H.J. Kim and Y.G. Kweon: "Elastic Modulus of Plasma-Sprayed Coatings Determined by Indentations and Bend Tests," *Thin Solid Films*, 1999, 342, pp. 201-06.
19. W.D. Kingery, H.K. Bowen, and D.R. Uhlmann: *Introduction to Ceramics*, 2nd ed., John Wiley & Sons, New York, 1976.
20. R.G. Munro: "Effective Medium Theory of the Porosity Dependence of Bulk Moduli," *J. Am. Ceram. Soc.*, 2001, 84(5), pp. 1190-02.
21. M.A. Camerucci, G. Urretavizcaya, and A.L. Cavalieri: "Mechanical Behavior of Cordierite and Cordierite-Mullite Materials Evaluated by Indentation Techniques," *J. Eur. Ceram. Soc.*, 2001, 21, pp. 1195-1204.
22. A.P. Roberts and E.J. Garboczi: "Elastic Properties of Model Porous Ceramics," *J. Am. Ceram. Soc.*, 2000, 83(12), pp. 3041-48.
23. N.N. Nemeth and J.P. Gyekenyesi: "Probabilistic Design of Ceramic Components with the NASA/CARES Computer Program" in *Engineered Materials Handbook, Vol. 4: Ceramics and Glasses*, S.J. Schneider, ed., ASM International, Materials Park, OH, 1991, p. 700-08.
24. C.K. Lin and C.C. Berndt: "Statistical Analysis of Microhardness Variations in Thermal Spray Coatings," *J. Mater. Sci.*, 1995, 30, pp. 111-17.